CIMAC CONGRESS 25
ZURICH, MAY 19 – 23, 2025

2025 | 527

Manufacturing of stainless components for alternative fuel systems applications

Fuel Injection & Gas Admission and Engine Components

Alkan Göcmen, PETER FUCHS TECHNOLOGY GROUP AG

Fabian Bartholdi, PETER FUCHS TECHNOLOGY GROUP AG
Frank Wrona, PETER FUCHS TECHNOLOGY GROUP AG
Stephan Ramjoue, PETER FUCHS TECHNOLOGY GROUP AG
Robin Reichmuth, PETER FUCHS TECHNOLOGY GROUP AG

ABSTRACT

The use of alternative fuels like methanol and ammonia for internal combustion engines is changing the boundary conditions for the layout of the pipeline system between pump and injectors as well as for the design and manufacturing of sub-components needed. The new boundary conditions are characterized by the need for larger bored fuel lines and by the need for stainless steels for the manufacturing of the fuel conveying sub-components. This study deals with the application of radial forging for manufacturing of cold formed fuel lines made of an austenitic stainless steel of the type 316L (1.4404) and intended for fuel system applications with system pressures up to 700 bar. This study further deals with the experimental verification of residual stresses brought in by cold forming and/or autofrettage and the experimental verification of the effect of residual stresses on high cycle fatigue limits of fuel lines. Finally, this study deals with the identification of a suitable stainless steel alloy that can be case hardened to attain a superior combination of surface hardness and corrosion resistance while providing a good combination of strength and toughness in the core as demanded for highly loaded components subject to wear.

Cold forming of pipes has been explored with reference to two aspects: (1) raising the strength of pipes made of higher corrosion resistant austenitic stainless steels, which are not hardenable by heat treatments, but through work (strain) hardening and (2) reduction of the bore diameters at the ends of fuel lines in order to facilitate metal to metal sealing of large bored fuel lines. Solution nitriding applied to martensitic stainless steel has been explored as a mean to enhance surface hardness and corrosion resistance of hardenable steel grades that offer an inherent good combination of strength and toughness in the as quenched condition.

Radial forging of seamless pipes or gun drilled pipes made of 316L stainless steels is demonstrated for the manufacturing of work hardened pipes and/or for the reduction of bore diameters at the ends of fuel lines. The development and redistribution of residual stresses during cold forming and autofrettage is studied by continuously measuring the elasto-plastic expansion of the tube diameter during pressurization of sample pipes up to the autofrettage pressures. Changes in the pressures at which pipe expansion becomes inelastic (flow-pressure) are correlated to residual stresses brought in by cold forming and in subsequent autofrettage treatments. While cold forming is shown to reduce the flow pressure due to residual tensile stresses, autofrettage at higher pressures is shown to bring the flow pressures back to values that can be calculated for a work hardened pipe without residual stresses. Accordingly, it is demonstrated that work hardening can be used to maximize the applicable autofrettage pressures and by the way the pressure at which pipes start to deform plastically.

It is shown by high cycle fatigue tests that the pressure pulsation amplitude for an endurable number of 5 million cycles of a commercially available pipe made of an austenitic stainless of type 316L with OD/ID-ratio of 2 and finished by autofrettage at 2,000 bar is limited to about 800 bar. This pressure pulsation limit can be enhanced to 1,900 bar by cold forming and a subsequent autofrettage treatment at 5,000 bar. The same fatigue resistance has been verified for a cold formed austenitic stainless steel pipe made of 316L in which the bore diameter at both ends were reduced by a factor of 2.

The case hardening opportunity of martensitic stainless steels by solution nitriding has been demonstrated on a novel alloy, which is based on 13wt.-%Cr, 3wt.-%Ni and 0.15wt.-%C and which was produced as a trial melt of 10 kg in a vacuum melting furnace. Its ability for case hardening has been demonstrated by a solution nitriding treatment in a vacuum furnace at 1,100°C and an applied nitrogen pressure of 1,000 mbar. The alloy reaches a surface hardness of 600HV and an electro-chemically measured pitting corrosion potential comparable with a 316L stainless steel, while core properties are characterized by a tensile-strength of 1365MPa and an elongation A5 of 14.7%.

1 INTRODUCTION

For internal combustion engines with carbon neutral or carbon free emissions the use of methanol or ammonia as a fuel is currently being considered. Accordingly, the fuel system is to be adapted to the physical and chemical characteristics of these fuels. The change in fuel from diesel to synthetic fuels changes the boundary conditions with respect to the layout of the fuel system, the materials and with respect to the design of the sub-components within the fuel system.

Two new trends seen in the design and material selection for methanol and ammonia conveying fuel system components are the increase of the bore diameters in the pipeline system and the increasing demand for stainless steel alloys. These two changes in boundary conditions are to be considered in regard to design guidelines, selection of stainless steel alloys and semi-finished products, finishing technologies like heat-treatment and autofrettage, and component testing for a safe application of the products at the end user. Putting this puzzle together is the main topic of this study.

Two tasks are particularly addressed in this study: (1) the use of austenitic stainless steels for design and manufacturing of fuel lines for application at fuel system pressures of around 700bar and (2) case hardening of stainless steel alloys for components subject to wear.

Austenitic stainless steels are not hardenable by heat-treatment. Work hardening by cold forming is the only way to increase strength in this class of steels. The use of radial forging, which is considered in the following study, is of particular interest here, because it does not only provide an opportunity for work hardening but also provides a new design opportunity, which emerges from a flexible adaptation of the outer and inner diameter of the pipe to geometrical boundary conditions specific to engine layout and component interfaces. With respect to that, autofrettage, which means pre-stressing a pipe at internal pipe pressures far above the operating pressure of the fuel system, is suggested to be of high relevance: not only for the built-up of desired compressive stresses but also for redistribution and elimination of detrimental, residual tensile stresses, which are brought in by cold forming. For the experimental determination of the effect of the residual stresses on fatigue life two new types of high pressure test-rigs have been engineered and built in home: (1) for the measurement and analysis of the internal pressure - strain characteristics of a pipe with and without residual stresses (2) for the measurement of fatigue life of tubular components under high, pulsating pressures. The use of radial forging for work hardening and cold forming of pipes along with the test-rigs (1) and (2) just introduced before forms the technological basis for the manufacture and the assessment of the mechanical properties of formed fuel lines made of stainless steels.

Unlike low alloyed steels there are no stainless steel alloys available that are specifically designed for case hardening by thermo-chemical diffusion processes that offer to adjust a hard surface with high corrosion resistance while leaving a strong but ductile structure in the core of a product. Solution nitriding, which has emerged from research on high nitrogen steels, is a heat treatment method that is seen to be of high relevance for case hardening of stainless steel alloys [1]. However, stainless steel alloys, which are suitable for case hardening by solution nitriding have not yet been developed and introduced to the market. In this study a novel alloy, which is suitable for case hardening by solution nitriding, is presented. This alloy is designed to meet fundamental requirements to a case hardenable stainless steel alloy in terms of surface hardness and corrosion resistance along with beneficial core properties in terms of strength and ductility.

2 OBJECTIVES

2.1 Design boundary conditions

The design boundary conditions and the various design tasks to be completed in the integration of a pipeline system, which connects the high pressure pump (pressure generator) with the injectors (fuel consumers), has been discussed at the CIMAC CONGRESS held in Helsinki 2016 with special reference to diesel common rail engines [2]. With the planned move from diesel to synthetic fuels like methanol or ammonia the bore of fuel lines is being enlarged to compensate for the lower energy density of these fuels as well as for the lower fuel systems pressure. The current trend reveals an increase of the bore diameter of fuel lines typically by a factor of 2 and more as compared to a diesel common rail engine with comparable cylinder bore dimensions and engine power output. Accordingly, more space has to be provided for the integration and connection of the various sub-components of a pipeline system like fuel lines, connection blocks, accumulators, pressure sockets and connectors. An increase in the bore diameter consequently results in an increase of the sealing diameter at the connecting interfaces. As depending on the material strength of the pipe sufficient wall thickness has to be provided to prevent excessive plastic deformation of the pipe ends and premature component failure by fatigue.

There is an opportunity to reduce the sealing diameter of fuel lines by reducing their bore diameter through cold forming (figure 1), which would facilitate sealing of the fuel lines. Here a higher safety factor for sealing can further be expected from the higher material strength provided by the work hardening of cold formed pipe sections.

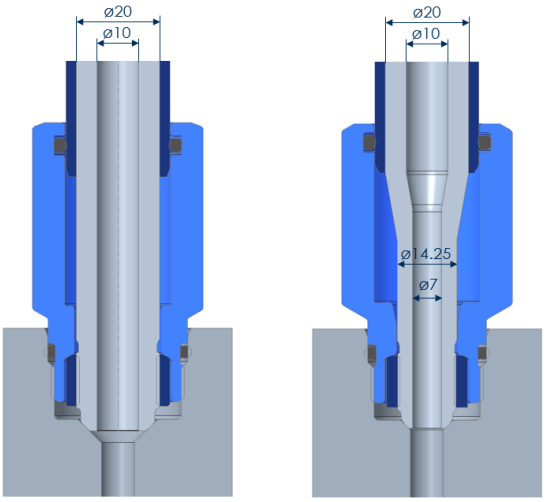

Figure 1. Illustration of a sealing connection provided by a reduction of the bore diameter at the end of the fuel line.

2.2 Mechanical boundary conditions

2.2.1 Deformation of pipes under internal pressure

The piping of fuel systems is elastically stressed under normal operation conditions. Tangential stress σ_t and radial expansion Δr_x at a radius r_x can be calculated using elasticity theory of internally stressed pipes with inner diameter $2r_i$ and outer diameter $2r_a$ as follows:

$$\sigma_t = p_i * \frac{r_i^2}{r_o^2 - r_i^2} * \left(\frac{r_o^2}{r_x^2} + 1\right) \quad (1)$$

$$\Delta r_x = \frac{p_i * r_x * r_i^2}{E*(r_a^2 - r_i^2)} * \left[\frac{r_i^2}{r_x^2} * (1 + \nu) + 1 - \nu\right] \quad (2)$$

In equation (2) E denotes Young's modulus and υ Poisson's ratio. Equation 2 is applicable up to internal pressures p_i at which a pipe starts to deform plastically. High pressure pipes are frequently finished by pressurization by a process called autofrettage. In this process pre-stressing occurs beyond a so called internal flow pressure $p_{i,f}$ at which pipes deform plastically starting from the bore and spread out towards the outer diameter of the pipe. After de-loading a compressive residual stress σ_s remains that reduces tangential stresses in a sub-sequential pressure built up. Equation (3), which is based on the maximum shear stress hypothesis, can be used for the calculation of the flow pressure $p_{i,f}$ at which plastic deformation at the bore surface of a material with yield-strength $R_{p0.2}$ starts.

$$p_{i,f} = \left(\frac{R_{p0.2}}{2}\right)\left[1 - \frac{r_i^2}{r_o^2}\right] \quad (3)$$

The occurrence of a residual stress σ_s within the pipe is expected to increase or to decrease the flow pressure depending on whether it is of compressive or tensile nature. As a first approximation one may assume that the change in flow pressure is directly correlated with the change in the tangential elastic stress, hence:

$$\Delta p_{f,i} \sim \Delta\sigma_t \approx \sigma_s \quad (4)$$

The practical implication of approximation (4) is the opportunity to estimate any residual stress of a straight pipe from an analysis of a pressure - expansion curve, which can be measured by continuous recording of radial expansion and pressure during pressurization of a pipe as shown in figure 2.

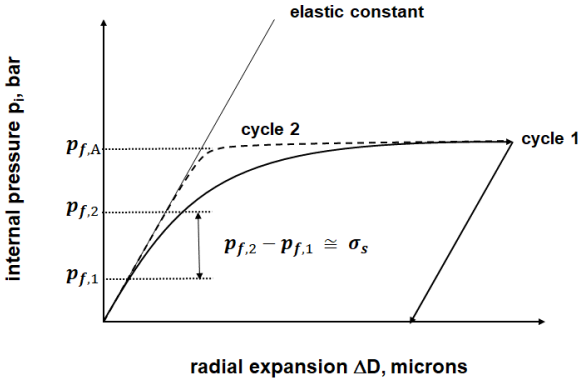

Figure 2: Representation of a pressure-expansion curve. In this graph cycle 2 follows subsequently to cycle 1.

In figure 2 the application of cycle 1 is expected to increase the flow pressure $p_{i,f}$, which is due to the generation of a compressive residual stress during the de-loading phase in cycle 1. Figure 2 also suggests that the curve will asymptotically approach a pressure $p_{f,A}$ at which the plastic deformation would reach the outer diameter of a pipe (full autofrettage), whereas in this case it is for reasons of simplicity assumed that the pressure $p_{f,A}$ is not affected by the residual stress in the bore introduced by cycle 1. Equation (5), which is also based on the maximum shear stress hypothesis,

can be used for the calculation of the pressure for full autofrettage.

$$p_{f,A} = R_{p0.2} * ln\left(\frac{r_o}{r_i}\right) \quad (5)$$

Depending on the thermo-mechanical pre-history of any tubular product some residual stress - being of compressive or tensile nature - may be left. Accordingly, the measurement of a pressure-expansion curve according to figure 2 provides a mean to estimate the magnitude of this residual stress.

2.2.2 High cycle fatigue (pressure pulsation) resistance of pipes

Pulsating pressures still well below the flow pressure of a pipe according to equation (3) can cause pre-mature failure through mechanical fatigue under pulsating pressure conditions. Since the stress is highest in the bore of a pipe according to equation (1) fatigue cracks are expected to initiate on the bore surface. A limiting stress for high cycle fatigue can be estimated by the approximation

$$\sigma_f \approx 0.4 * R_m \quad (6)$$

wherein R_m denotes the tensile-strength of the material. Accordingly, high cycle fatigue is to be expected when tangential stresses according to equation (1) exceed the high cycle fatigue stress according to approximation (6). One may expect pre-mature fatigue failure still below this theoretical fatigue limit under the following three circumstances: (1) bore surface is excessively rough, corroded or contains cracks, (2) the environment (fluid) is excessively corrosive and (3) the bore of the pipe has residual, tensile stresses that add to the stress provided by external loadings. The role of residual stresses is of particular relevance here since they have a big effect on fatigue limit and they are not visible by ordinary inspection methods. As mentioned just before residual tensile stresses at bore surfaces will contribute to the total elastic stress and thereby reduce the endurable, pulsating pressure limit, while compressive stresses, which can be introduced by autofrettage, will increase the resistance to fatigue by pressure pulsations. Known residual stresses have to be added to the calculated tangential stresses to predict the fatigue limit as follows:

$$\sigma_{t,tot} = \sigma_t + \sigma_s \geq 0.4 * R_m \quad (7)$$

Figure (3), in which total tangential stress $\sigma_{t,tot}$ for a pipe with r_o = 10mm and r_i = 5mm is plotted as a function of internal pressure p_i, illustrates the impact of various residual stresses on the fatigue limit using the following two cases for a pipe A and a pipe B. Both pipes A and B shall have the same yield-strength $R_{p0.2}$ of 800MPa and a tensile strength R_m of 1000MPa and the same OD/ID-ratio of 2. In the absence of any residual stress plastic deformation under internal pressure is expected to occur at an internal pressure $p_{i,f}$ of 3042bar (equation 3). The critical pressure amplitude for fatigue is assessed to be 2400bar, which is based on the calculation of the pressure at an elastic stress (equation 1) given by the approximation 0.4*R_m = 400MPa (equation 6). As discussed in section 2.2.1 the measurement of a flow-pressure well below 3042bar would be an evidence for the presence of a tensile residual stress. In case A a flow pressure $p_{i,f}$ of 1200bar is measured, which based on equation 1 and 4 suggests a tensile residual stress of 200MPa. The new fatigue limit referring to case A is accordingly reduced from 400MPa to 200MPa and the fatigue limiting pressure amplitude is reduced from 2400bar to 1200bar. In case B the component is pre-stressed by autofrettage, that increased the flow-pressure $p_{i,f}$ from 3042bar to 3600bar as schematically illustrated in figure 2. Accordingly, a residual, compressive stress of 200MPa is to be assumed, which would increase the fatigue limit by 400MPa to 600MPa and by the way the endurable pulsating pressure amplitude from 2400 bar to 3600bar. Case A and B illustrate the sensitivity of the endurable pressure pulsation amplitude upon residual stresses in a pipe with an OD/ID-ratio of 2. The knowledge of this residual stress is fundamental for a proper assessment of the fatigue limit of a pipe.

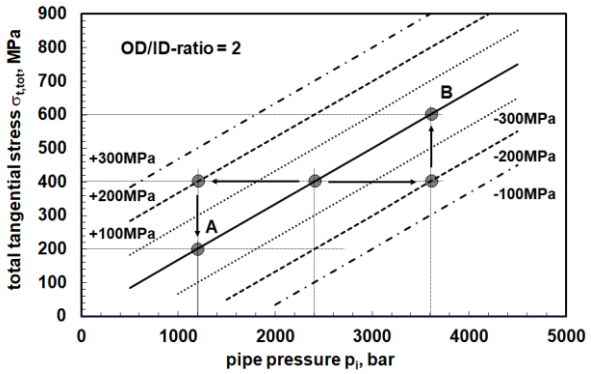

Figure 3: A tensile residual stress of +200MPa (case A) reduces the limiting pressure amplitude to 1200bar whereas a compressive residual stress of -200MPa (case B) enhances the limiting pressure amplitude to 3600bar.

2.3 Materials and Manufacturing

2.3.1 Metallurgical boundary conditions

Special environmental conditions may necessitate the use of stainless steels for manufacturing of the

sub-components of a pipe line system as long as no alternative and adequate protection against corrosion during operation and maintenance can be provided. The term stainless steel refers to any steel grade that provides a minimum resistance to rusting. This resistance to rusting is physically provided by a passive layer that forms on the steel surface when chromium in the alloy reacts with oxygen from the environment and a minimum of 12% chromium is known to provide sufficient resistance against rusting in a clean environment, as we may found inside living spaces. Unlike ordinary rusting that spreads out on a metal surface local attack of the passive layer favors a localized corrosion that can promote nucleation and growth of cracks of loaded components. The sensitivity of a steel to localized corrosion can be electro-chemically characterized by a measurable pitting corrosion potential E_{pit}, which serves a basis for comparing and ranking of stainless steel grades with respect to pitting corrosion resistance. For this pitting corrosion potential a pitting resistance equivalent number (PREN) has been established by metallurgists to correlate the chemical composition of a stainless steel grade in weight percentages with a pitting corrosion potential [3]:

$$PREN = \%Cr + 3.3\%Mo + 16\%N \qquad (8)$$

Among the available steel grades, 316L stainless steel with DIN 1.4404, which contains 17.5%Cr and 2.25%Mo to provide a PREN of 25, is considered as a benchmark for adequate corrosion resistance of loaded components in industrial environments. The availability of seamless and thick-walled pipes up to an OD/ID-ratio of 2 makes grade 316L a favored candidate for manufacturing of higher corrosion resistant high pressure fuel lines.

Available pipes made of 316L stainless steel are typically finished by means of a solution heat treatment leaving a semi-finished product with a yield-strength $R_{p0.2}$ as low as 200MPa and a tensile-strength R_m as low as 500MPa. These types of stainless steels are not hardenable by heat treatment and work hardening by cold forming is the only possibility to increase the base strength of semi-finished products. Figure 4 represents the work hardening characteristic of a 316L (1.4404) stainless grade that results from straining of a bar. A preferred tensile-strength R_m of 1000Pa is shown to be achieved by stretching of a bar or pipe made of a 316L stainless steel by a factor L/L_0 of about 1,3.

Less corrosion resistant grades with 12 to 15% chromium are hardenable by martensitic transformation to attain hardness levels up to about 58-62HRC. Grades within this type of stainless steels are being used for manufacturing of highly stressed stainless components subject to wear and PREN values of 24 to 25 are achievable with high nitrogen alloyed grades like X30 CrMoN 15 1 (1.4108).

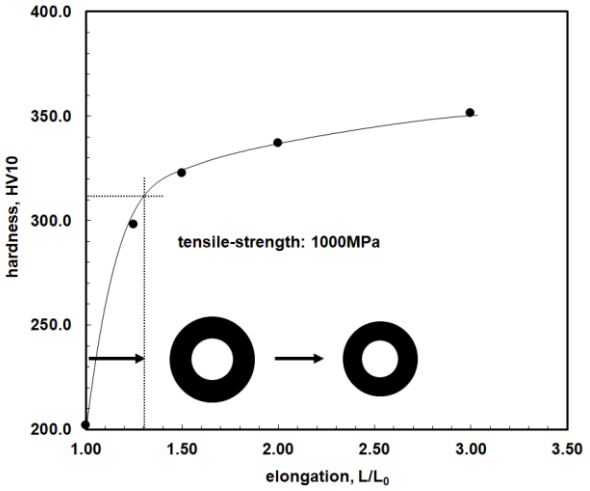

Figure 4: Strain hardening of 316L produced by cold, radial forging of a bar. The figure further illustrates to which extend a pipe has to be deformed by reducing outer diameter (OD) and inner diameter (ID) with an OD/ID-ratio of 2 to end up with an elongation L/L_0 of 1,3 needed to adjust a tensile-strength of 1000MPa with 316L.

When it comes to heat treatment it has to be borne in mind that good corrosion resistance of stainless steel is achieved in the solution heat-treated or quenched hardened condition only. Annealing at intermediate temperatures degrades corrosion resistance by so-called sensitization reactions, in which nucleation of chromium-rich carbides or nitrides leave a continuous, chromium impoverished zone along grain boundaries. As a consequence of that, and unlike the low alloyed grades that have virtually no corrosion resistance, there is no opportunity to reduce residual stresses in cold-worked austenitic stainless steels by a stress relief treatment at intermediate temperatures to maintain some of the work hardening brought in by cold forming. The only applicable heat treatment that eliminates un-desired residual stresses or a sensitized microstructure is a solution annealing treatment that re-establishes the low strength level and the corrosion resistance of solution annealed grades. This sensitization of stainless steels is the main reason why classical carburizing, nitriding or carbo-nitriding processes, which are widely applied to low alloyed grades, are not applicable to any stainless steel.

For some applications case hardening providing a well-balanced core in terms of strength and ductility and a corrosion resistant and deep hardened surface may be demanded for highly loaded

components subject to wear. In low alloyed steels this is very effectively and economically being realized by using a more or less non-hardenable grade that becomes hardenable on the surface by carbon and nitrogen up-take, which is commonly known as carburizing or carbo-nitriding. The same is potentially applicable to stainless steels provided that carbon and nitrogen up-take occur at a temperature that is well above the temperature at which sensitization occurs. Nitrogen appears to be the preferred atom for that mainly due to its higher solubility in the austenitic state of martensitic hardenable stainless steels from where martensite is produced upon quenching. Any alloy that provides a good balance of corrosion resistance, strength and toughness in the as-quenched condition thus becomes a candidate for case hardening by solution nitriding [4]. This heat treatment opportunity is illustrated in Schaeffler's diagram in figure 5, which is used by metallurgists for an approximate prediction of a microstructure given a defined alloy composition.

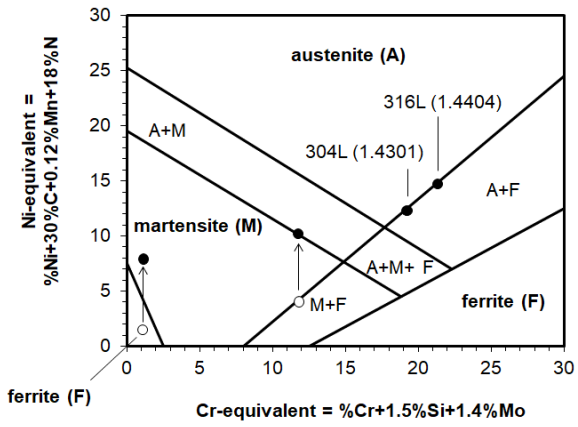

Figure 5: Schaeffler's diagram for the prediction of the base structure as depending upon chemical composition. On the left side in the ferritic field a classical case hardenable alloy is represented (open circle), which upon carbon uptake by carburizing (full circle) enables the surface to harden through a martensitic transformation. On the right side of the martensitic field a stainless steel is represented, which is just fully hardenable by martensitic transformation (open symbol) whereas a limited nitrogen up-take (full symbol) can intensify the martensitic hardening reaction without scarifying the alloy's capability for martensite hardening.

In figure 5 a hypothetical, martensitic alloy with 12%Cr and 4%Ni is shown, which is able to take up higher quantities of nitrogen without giving up the alloy's capability for martensitic hardening. The achievable hardness, as depending upon carbon and nitrogen content, can within certain limits be predicted by the following, empirical approximation:

$$H_M[HRC] \approx 20 + 60\ x\ \sqrt{\%C + \%N} \qquad (9)$$

Putting equation (8) and (9) together suggests that any nitrogen up-take on the surface will not only improve pitting corrosion resistance but also the surface hardness of martensitic hardenable grades. This so called solution nitriding, which can be realized in a vacuum furnace under a controlled nitrogen partial pressure and quenching with an over-pressure of nitrogen, is suggested to provide a perspective for the development of case hardenable stainless steels. The metallurgist's task is to identify a suitable alloy, that is able to attain a good combination of strength and toughness in the as quenched state and that is still able to dissolve high quantities of nitrogen at hardening temperatures without losing the ability of the hardenable base alloy for an effective martensitic hardening reaction [4].

2.3.2 Manufacturing

2.3.2.1 Pipe manufacturing – Seamless pipes of grade 316L (1.4404) with sufficiently good bore surface quality are available in the soft (solution annealed) condition as hydraulic pipes with a diameter ratio OD/ID of up to 2. This combination of strength and wall thickness limits the endurable pressure under pulsating conditions. As described in the previous section pipe strength can be increased by work hardening through cold forming. The most economical way to accomplish that is through cold forming of an available seamless pipe. Alternatively, bars can be work hardened by cold forging from where the desired pipes can be fabricated by gun drilling. The length of a pipe that can be achieved by gun drilling is limited to a length (L) to inner diameter (ID) ratio of about L/ID≤100. Fabrication of pipes with higher L/ID-ratio accordingly necessitates the addition of a cold drawing or a cold forging process. In figure 6 the process for cold forming by radial forging, which is used in this study, is illustrated. In this process the outer diameter OD as well as the inner diameter ID of a pre-fabricated pipe are reduced by hammer strokes, whereas the ID can be kept within a narrow tolerance by using a precisely finished mandrel within the pipe. During the cold forging process the OD/ID-ratio increases until the bore touches the mandrel. Accordingly, the radial forging process does not only allow to increase the strength of a pipe by work hardening but also by increasing the OD/ID-ratio.

Finally, radial forging can also be applied to pipe ends only. On that way OD and ID can be reduced to facilitate the connection to the adjacent component. For a good bore surface finish bore

reduction is currently being limited to a factor ID_{before}/ID_{after} of 1,5. Within this limit an elongation L/L_0 of up to 2.25 can be realized for manufacturing of work hardened pipes.

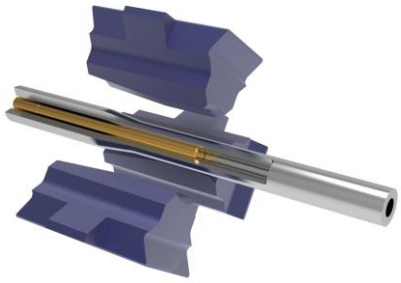

Figure 6: Radial forging is a way to stretch pre-fabricated pipes. Narrow ID tolerances with a fine bore finish are realized by forging the bore onto a precisely finished mandrel (gold colored).

2.3.2.2 Finishing processes – Solution annealing at temperatures above 1000°C is the applicable heat treatment of austenitic stainless steel to eliminate residual stresses and/or to re-establish the corrosion resistance of a degraded microstructure. Autofrettage is the alternative finishing process for control of internal stresses. While the dimensions of available heat treatment equipment, in particular vacuum furnaces, become a limiting factor for solution annealing of long and/or bulky components, autofrettage can be applied to long and bent fuel lines. The main advantage of autofrettage as compared to a solution annealing treatment however is that the initial strength level is maintained.

As introduced in the previous section case hardening of stainless products can be attained by identification of a hardenable base alloy, which is thermodynamically suitable for the application of a solution nitriding process. While nitrogen up-take can be adjusted by control of nitrogen partial pressure at solution nitriding temperatures, which follows Sievert's law according to

$$\%N \sim \sqrt{p_{N_2}} \qquad (10)$$

the hardening depth can be adjusted by the holding time at the temperature at which nitrogen up-take occurs. Same as with all stainless products these products are to be rapidly quenched with an adequate nitrogen over-pressure to prevent sensitization during the cooling step.

3 EXPERIMENTALS

3.1 Raw materials

Materials used for manufacturing and testing are listed in table 1 along with their mechanical properties and chemical compositions according material certificates. Seamless pipes and bars made of 1.4404 (316L) used for manufacturing of sample preparation have been procured from stockists.

AP2 is a homemade steel alloy designed for case hardening by solution nitriding. A heat of 10kg of AP2 was melted at a temperature of 1600°C. The ingot with a diameter of 72mm was homogenized and subsequently open die forged to diameter 45mm in the temperature range between 1200 and 950°C and radially forged on a GFM SKK10 at 800°C to diameter 25mm. These bars were annealed at 800°C for two hours, air cooled and finally tempered at 200°C for 2 hours that resulted in a hardness of 342HV30. Case hardening trials were conducted after machining the bars to diameter 22mm.

Table 1. characteristics of materials used for sample preparation

alloy	**1.4404**	**1.4404**	**AP2**
test samples[1]	A, C	B, D	
raw product[2]	SP	bar	bar
OD/ID [mm]	20/10	25	22
mechanical properties			
$R_{p0.2}$ [MPa]	293	451	
R_m [MPa]	610	631	342HV
A5 [%]	58	45	
chemical composition in wt. %			
Fe	bal	bal	bal
C	0.021	0.022	0.15
Si	0.41	0.45	0.49
Mn	1.72	1.27	0.71
P	0.04	0.04	< 0.003
S	0.008	0.005	0.005
Cr	16.68	17.05	13.33
Ni	10.01	10.03	3.09
Mo	2.01	2.01	0.018
N	0.08	0.04	< 0.05

[1] see product designations in table 2
[2] SP stands for a seamless pipe

3.2 Test samples

Table 2 lists the various, tubular test samples that differ with respect to raw material used, dimensions, manufacturing process and the finishing method applied.

Table 2: sample characterization

sample	processing characteristics
A-SP	seamless pipe (as delivered)
A-SP-AF	A autofrettage finished
B	gun drilled and forged pipe
B-AF	B autofrettage finished
C[1]	accumulator pipe
C-AF	C autofrettage finished
C-SA	C solution annealed
C-SA-AF	C-SA autofrettage finished
D[2]	accumulator pipe
D-AF	D autofrettage finished

[1] A-SP is the raw material used
[2] B is the raw material used

Accumulator pipes of type C and D have been cold formed by radial forging to the dimensions shown in figure 7.

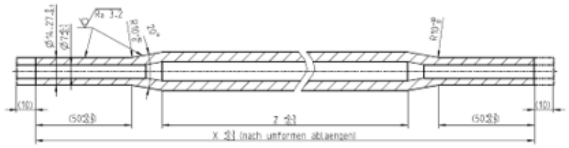

Figure 7: accumulator pipe dimensions

Type C accumulator end is thus produced reducing the bore of a seamless pipe at both ends.

Type D accumulator pipe in turn is produced by gun drilling of a bar, cold forming along the full length and final reduction of the bore at both ends.

3.3 Manufacturing and finishing conditions

3.3.1 Gun drilling

Gun drilling with single-lip tools were used for preparation of type B and D samples. On that way semi-finished pipes with outer diameter (OD) 25mm and inner diameter (ID) 13mm were produced for further processing by cold forming of B & D samples.

3.3.2 Radial forging

GFM SKK10 radial forging machine was used for cold forming of B, C & D samples. The machine consists of a forging unit with 4 up-right hammers as shown in figure 6, which are synchronized and have a fixed stroke of 7 mm. There are two feed units with manipulators in front and behind the forging box, each with a travel of 3000 mm, which can accommodate the work piece and/or internal tools (mandrels). All axes and the diameter of the hammers are freely programmable. The bars or tubes are cycled in their rotation through the hammering unit by the manipulator.

For cold forming of high pressure pipes a seamless or gun drilled pipe is loaded on the manipulator on side 1 whereas the inner tool (mandrel) is mounted on side 2. The hammers are opened and the blank is moved onto the inner tool. The hammers pierce and the work piece is forged by pulling over the mandrel. On that way gun drilled bars with OD25/ID13mm were converted into work hardened pipes with OD20/ID10mm (type B samples). The application of this cold forging enables to maintain the pre-scribed ID tolerance of +/- 0.1mm and an extraordinary surface finish of the bore is provided by a precisely ground and polished mandrel.

For cold forming of accumulator pipes samples C & D semi-finished pipes with OD20/ID10mm were loaded on side 1, whereas an inner tool (mandrel) was mounted on side 2. The hammers are set to the target diameter of OD14.3mm while the mandrel with diameter 7mm is positioned under the hammers.

3.3.3 Heat treatments

For the sole purpose of a stress relief treatment cold formed accumulator pipes of type C-SA were solution annealed in a vacuum furnace at 1050°C for 10 minutes with a subsequent gas over-pressure quenching with 6bars.

Case hardening of AP2 bar samples was carried out in a vacuum furnace at 1100°C for 1 hour at an applied nitrogen partial pressure of 1000mbar. The specimens were subsequently quenched with a gas over-pressure of 6bar and finished by deep freezing at -80°C for 2h and a final tempering treatment at 160°C for 4 hours.

3.3.4 Autofrettage

Samples A-SP-AF, B-AF, C-AF, C-AS-AF and D-AF were finished by autofrettage as indicated by the designation AF. The applied autofrettage pressure is naturally limited by the pressure where full autofrettage occurs according to equation 5. For solution annealed sample C-AS-AF further reduction of the autofrettage pressure as compared

to specimen A-SP-AF was necessary due to excessive deformation of the cone ends of that solution annealed (soft) sample. Table 3 lists the applied autofrettage pressures. Note here that the autofrettage pressure of accumulator pipe D-AF is much higher than applied for accumulator pipe C-AF. This was made possible by the higher strength of cold forged OD20mm section in samples B-AF and D-AF.

Table 3: autofrettage parameters

sample	autofrettage pressure
A-SP-AF	2000-2150bar
B-AF	5000bar
C-AF	2150bar
C-SA-AF	1800bar
D-AF	5000bar

3.4 Testing conditions

In house engineered and built test-rigs were used for the measurement of pressure-expansion curves and for high cycle fatigue tests.

3.4.1 Pressure-expansion curves

An autofrettage work station is used for pressure generation and the test specimen is connected directly to the pressure pump in an upright position. A displacement measuring system with two opposing sensors touch the specimen (figure 8) and allow continuous recording of radial expansion in the micro-meter range during a continuous pressure built-up.

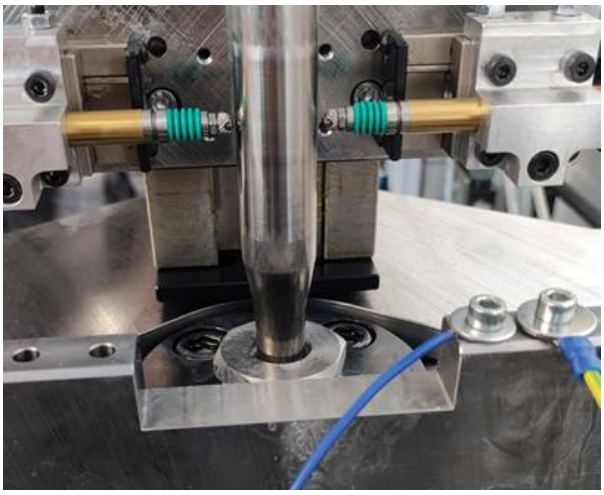

Figure 8: experimental set-up for pressure-expansion curve measurements with displacement sensors (green colored)

3.4.2 High cycle fatigue

A new type of fatigue test-rig has been developed that bases on a mechanical crank drive with a crosshead, which is coupled with a high-pressure piston. The stroke can be adjusted from 0-55 mm during operation via a servo drive using an adjustment mechanism. The test specimens are thus being tested sinusoidal and form an almost closed system. This means that a large proportion of the energy from the pressure reduction can be utilized again, making the systems very energy-efficient.

This fatigue-test rig is designed for pressures up to 4500 bar and 11 Hz.

The machine control system analyses the sine wave, regulates the system, counts the cycles and saves the data in a higher-level system.

Switch-off conditions are pressure difference, temperature curve, oil mist or number of cycles reached. The test-rig can be used in 24/7 operation.

In this study all fatigue test samples have been cycled between 100bar and a defined peak-pressure using a calibration oil as the pressurizing fluid.

3.4.3 Corrosion testing

The corrosion resistance of case hardened samples of alloy AP2 was investigated by means of polarization scans, which were taken up with an EC-pen that consists of two electrodes dipped in a reservoir of 0.5M NaCl. The pen-tip has a surface area of about 1.5mm^2 and the applied velocity was 5mV per second. All samples were tested in a polished condition.

4 RESULTS

4.1 Pipes

4.1.1 Material characterization

Cold forging of pipes results in work hardening. This is verified by hardness measurements along the axis of accumulator pipe samples C and D (figure 9). Sample D, in which the larger OD20mm as well as the smaller OD14.3mm was forged, shows higher hardness values than sample C. The increase of hardness from OD20mm to OD14.3mm of sample D is small as compared to sample C. On the cold forged cross section of OD14.3/ID7 sample C achieves 335HV, whereas sample D reaches 360HV. This is in accordance with previous strain hardening results made on cold forged bars (figure 4).

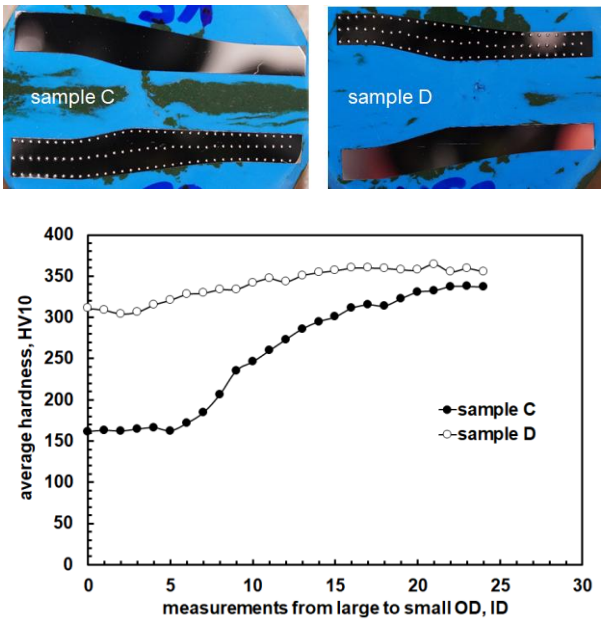

Figure 9: hardness distribution in accumulator pipes: sample C and D

The bore of as delivered seamless pipe A-SP with OD20/ID10mm is characterized by micro-cracks with a maximum depth of 62.7microns (figure 10, table 3). These cracks grow within the transition zone up to a depth of 99.2microns during cold forging of the accumulator pipe sample C. Interestingly, the smaller ID7mm in sample C with higher hardness shows cracks smaller in depth than in the larger ID10mm, which may indicate that existing cracks tend to align during forging in the direction of the bore axis. Gun drilled and forged accumulator pipe sample D shows shorter cracks in the larger ID10mm and transition zone but slightly deeper cracks in the smaller bore ID7mm.

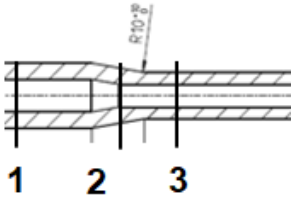

Figure 10: location of cuts for crack depth measurements

Table 3: overview of crack depth measurements

sample	**C**	**D**
location 1		
<d> [microns]	45.0	33.3
d_{max} [microns]	62.7	35.8
location 2		
<d> [microns]	64.3	53.1
d_{max} [microns]	99.2	59.2
location 3		
<d> [microns]	35.8	43.0
d_{max} [microns]	39.8	50.5

4.1.2 Mechanical properties of pipe samples

4.1.2.1 Tensile properties – Table 4 lists the mechanical properties of various pipe samples and cross sections as resulting from their processing pre-history:

Table 4: mechanical properties of as delivered and cold forged pipes

sample	Rp.0.2 [MPa]	Rm [MPa]	A5 [%]
A-SP (as delivered) seamless pipe OD20/ID10mm	293	610	58.1
B gun drilled & forged OD20/ID10mm	862	944	16.6
C seamless pipe forged OD14.3/ID7mm	939	1017	10.2

In Table 4 the tensile properties of A-SP serve as a reference for a standard seamless pipe (SP) made of 316L. Sample B is a cold forged tube that is made of a gun drilled bar with OD25/ID13mm cold formed to OD20/ID10mm as described in section 3.3.2. Sample C was manufactured by cold forging of seamless pipe A-SP with OD20/ID10mm to OD14.3/ID7, which results in an elongation L/L_0 of 1,93. Table 4 shows that strength increases while the ratio of $R_m/R_{p0.2}$ as well as elongation A5 decreases with increasing elongation L/L_0 during cold forming.

4.1.2.2 Pressure-expansion – Sample A-SP, B and C characterized in the previous section have been used for the measurement of pressure-expansion curves (figures 11a-c). Three successive pressurizing cycles are shown for each sample A-SP, B and C. The first cycle

characterizes the as manufactured material condition without autofrettage as defined by the designations A-SP, B and C for which the tensile properties listed in table 4 can be used to calculate flow pressure $p_{i,f}$ (equation 3) and the pressure for full autofrettage $p_{f,A}$ (equation 5). Cycle 2 is carried out subsequently after de-loading. Cycle 3, which followed in direct subsequence to cycle 2 was carried out in order to examine whether cycle 2 would result in a further change in flow pressure $p_{i,f}$ and pressure for full autofrettage $p_{f,A}$ that would be noted in cycle 3.

Radial-expansion should be elastic in the initial loading stage and in the de-loading stage as determined by Young's modulus (E=190-200GPa) and Poisson's ratio (ν=0.0.265-275). This is for all samples verified in the de-loading stage and for the 2nd and 3rd cycle in the initial loading stage. However, in the first cycle of sample A-SP, B and C an anomaly is observed that couldn't be explained so far, but is considered to be a purely experimental error. Flow pressure $p_{i,f}$ in cycle 1 has been determined by the onset of a deviation from the elastic slope as calculated based on Young's modulus and Poisson's ratio according to equation 2.

It is evident from figure 11a to 11c that the flow pressure $p_{i,f}$ increases from the first to the second cycle. A change of the flow pressure from cycle 2 to 3 appears to be negligible for this type of pipes, alloy and mechanical pre-history. It is further evident that work hardened sample B and C can be pressurized to much higher pressures than sample A-SP until full autofrettage occurs.

The decline of the pressure-expansion curve at high pressures reveals that the curve is approaching the pressure for full autofrettage. This is very evident from cycle 1 of sample A-SP in figure 11a and from cycle 1 of sample C in figure 11c. For sample B and all other cycles, the pressure level for full autofrettage could not be reached by continuous pressurization due to the given limitations of the pressure generator for a continuous pressure built up.

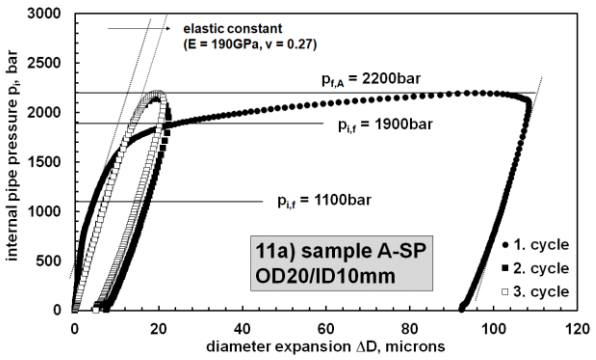

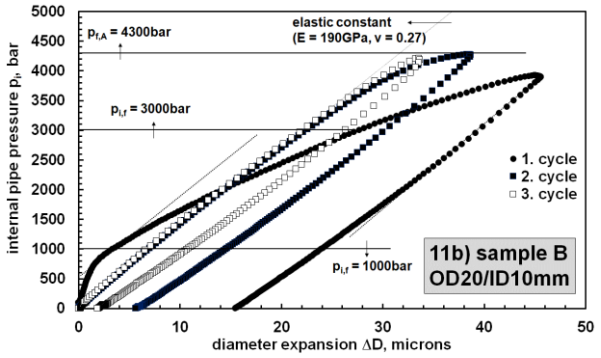

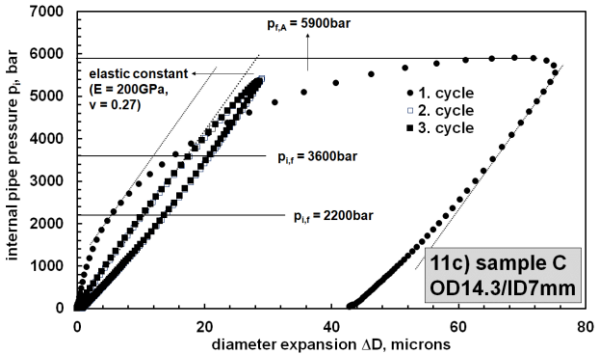

Figures 11a-c: representation of pressure-expansion curves for samples A-SP, B and C with underlying tensile properties listed in table 4.

4.1.2.2 High cycle fatigue – Table 5 lists results from high cycle fatigue tests for the as delivered seamless pipe A-SP and for the accumulator pipes C and D with the dimensions shown in figure 7. As described in section 3.3.1-2 these accumulator pipes were produced by radial forging of both ends of a seamless pipe (sample C, C-SA and C-SA-AF) or by radial forging of both ends from a gun drilled and radially forged bar (sample D-AF). Accordingly, the results of the accumulator pipes were compared with the results of the as delivered seamless pipe A-SP with and without autofrettage (AF) based on the pressure amplitude to reach 5 million cycles (5-M-cls pressure amplitude).

Table 5: overview of achieved 5-M-cls pressure amplitude

sample	$5x10^6$-cls pressure amplitude [bar]	safety factor for 700bar
A-SP	800	1.14
A-SP-AF	900	1.29
B[1]	600	0.86
B-AF	2100	3
C	600	0.86
C-SA	900	1.29
C-SA-AF	900	1.29
D	600	0.86
D-AF	2100	3

[1] extrapolated value

Accumulator pipe C made of seamless pipe A-SP showed premature failure at pressures above a pressure amplitude of 600bar. In the great majority of the investigated accumulator pipes cracks initiated pre-dominantly at the transition point from the larger bore ID10mm to the smaller bore ID7mm in location 2 as depicted in figure 10. The 5 million cycles pressure amplitude could be successfully increased to 900bar by a solution annealing treatment (SA). However, no further increase in the fatigue limit could be achieved by an additional autofrettage treatment (AF) at 2000bar. For a comparison as delivered seamless pipe A-SP provided a 5 million cycle pressure amplitude of 800bar. Here too, an autofrettage treatment applied to this pipe at 2000bar was able to increase the endurable pressure amplitude from 800 to 900bar only. Gun drilled and radial forged pipe with OD20/ID10mm has shown pre-mature failure at 900 and 800bars. The accumulator pipe D-AF, which was produced from a bar by gun drilling and radial forging of sample B doesn't fail up to a pulsation pressure amplitude of 2100bar.

4.2 Case hardening

4.2.1 Material characterization

Case hardening trial applied to alloy AP2 as described in section 3.3.3 resulted in a fully martensitic structure with former austenite grains in the range between 50 to 150 microns (Figure 10).

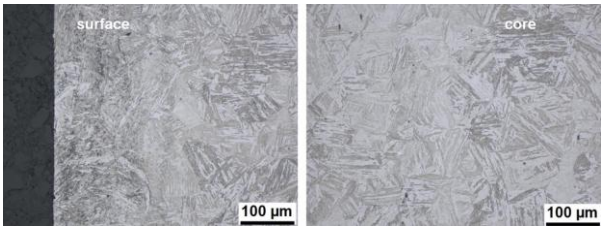

Figure 10: quenched and tempered microstructure of case hardenable steel AP2.

The surface hardness reaches 610HV0.3 and drops to a value of about 410 to 430HV0.3 of the core, which converts to a tensile-strength R_m of 1400MPa (Figure 11). The following mechanical properties were obtained from a tensile sample, which was machined out from the core area:

Yield-Strength $R_{p0.2}$:	1047MPa
Tensile-Strength R_m:	1365MPa
Elongation A_5:	14.7%
Contraction Z:	60%

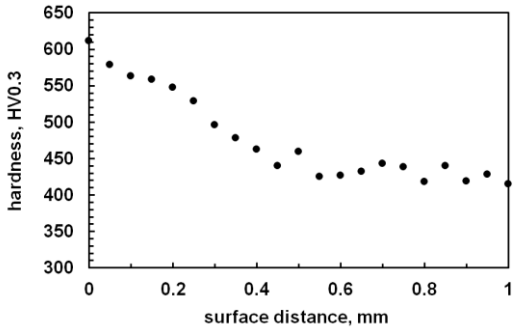

Figure 11: Hardness curve of cased hardened steel alloy AP2. The nitride hardening depth NHD was measured to be around 0.45mm.

4.2.2 Pitting corrosion resistance

Pitting corrosion resistance of AP2 has been assessed by means of polarization scans as described in section 3.4.3 on a polished surface. For AP2 a comparison is made between the core and the hardened surface. A further comparison is made with 1.4108 (Cronidur 30) with a surface hardness of 59HRC and with a stainless steel of the type 1.4404 (316L) in the as delivered (solution annealed) condition.

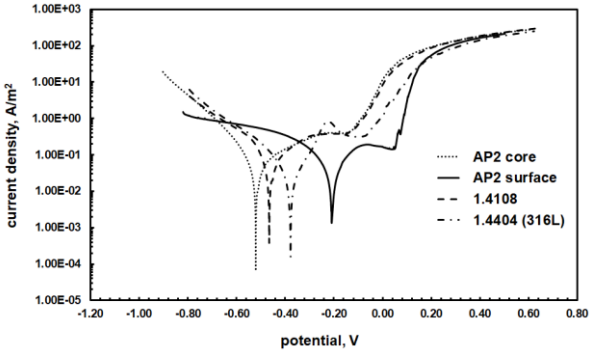

Figure 12: polarization scan of case hardened alloy AP2 in the core and on the surface in comparison with commercially available benchmarking alloys (hard 1.4108 and soft 1.4404)

The pitting corrosion potential representing the core of AP2 is -140mV and interestingly the same result was obtained for grade 1.4108. The pitting corrosion potential increases to 40mV on the case hardened surface of AP2, which appears to be still better than what was achieved for a commercially available austenitic stainless grade of 316L/1.4404 (-80mV).

5 DISCUSSION

5.1 Pipe performance

Results on the mechanical properties of pipes are compared with the theoretical predictions outlined in section 2.2 (table 6).

Table 6: Summary of pipe results

sample	**A-SP**	**A-SP -AF**	**C**	**C-AF**	**B**	**B-AF**
sample type	seamless pipe		accumulator pipe		drilled & forged pipe	
manufacturing process	as delivered		radial forging		gun drilling & radial forging	
pipe dimensions						
r_o [mm] (mid section)	10.0	10.0	10.0	10.0	10.0	10.0
r_i [mm] (mid section)	5.0	5.0	5.0	5.0	5.0	5.0
r_o [mm] (end section)	n.a.	n.a.	7.15	7.15	10.0	20.0
r_i [mm] (end section)	n.a.	n.a.	3.5	3.5	5.0	10.0
tensile properties						
yield-strength $R_{p0.2}$ [MPa]	316	316	937	937	862	862
tensile-strength R_m [MPa]	610	610	1019	1019	944	944
A_5 [%]	50.0	50.0	10.8	10.8	16.6	16.6
properties of pipes						
flow pressure calculated $p_{i,fc}$ [bar][1]	1185		3562		3233	
flow pressure measured $p_{i,fm}$ [bar][1]	1100	1900	2200	3600	1000	3000
pressure for full autofrettage calculated $p_{f,Ac}$ [bar][1]	2190	2190	6693	6693	5975	5975
pressure for full autofrettage measured $p_{f,Am}$ [bar][1]	2200	2200	5900	5900	4300	4300
estimated residual stress σ_s [MPa]	14	-119	228	-6	373	39
pipe fatigue properties						
fatigue strength 0.4Rm [MPa]	244	244	408	408	378	378
fatigue limit without residual stress [bar][1]	1464	1464	2700	2700	2266	2266
fatigue strength with residual stress [MPa][1]	230	363	180	414	5	339
fatigue limit with residual stress [bar][1]	1379	2180	1080	2483	29	2033
specimens used for fatigue testing	**seamless pipe**		**accumulator pipe**			
$5x10^6$-cls pressure amplitude measured [bar]	800	900	600	900[2]	600[3]	2100[4]

[1] For samples C and C-AF these properties were determined on pipes cold formed to AD14.3/ID7mm. For samples B and B-AF these properties were determined on cold formed section AD20/ID10mm.

[2] This result was achieved with a solution annealing treatment without autofrettage; an autofrettage treatment at 2000bar resulted in no further enhancement of the endurable pressure amplitude.

[3] This is estimated from pre-mature failures 1100bar (224.807 cycles) and at 900bar (415.700 cycles).

[4] The same result was also achieved for the cold forged accumulator pipe D-AF made of sample B.

For an untreated seamless pipe (A-SP) calculated flow pressure $p_{i,fc}$ for the onset of plastic deformation and the pressure for full autofrettage $p_{f,Ac}$ are found the be in good accordance with predictions of mechanical calculations (see section 2.2.1). The deviations are within an experimental error, which suggests that obtained pressure-expansion curves could be used to measure the flow pressure in the first cycle despite the anomaly observed in the initial stage. Even though the plastic properties of the pipe came out as expected and showing no evidence for a significant residual stress the achieved 5 million cycles pressure amplitude was distinctly below calculation (1379bar vs. 800bar). The application of an autofrettage shows an increase of the flow pressure from 1100 to 1900bar, which suggests that a compressive residual stress of 119MPa could be introduced by autofrettage at 2200bar. The addition of a compressive stress of 119MPa to sample A-SP in turn suggests an increase of the endurable pressure amplitude by 801bar. However experimental pressure amplitude could not be raised by more than 100bar to reach 5 million cycles. In summary, for an ordinary seamless pipe made of 316L a fatigue safety factor of 1.14 (800bar/700bar) can be assumed for an infinite number of start-up/shut-down cycles to and from an operation pressure of 700bars. This safety factor can only slightly be raised to 1.29 by finishing it with an autofrettage treatment at 2000bar.

In accumulator pipe C-SP the pressures for flow $p_{i,fc}$ and for full autofrettage $p_{f,Ac}$ were measured on a pipe A-SP that was cold forged from OD20/ID10mm to OD14.3/ID7mm. Both measured values are found to be distinctly below calculated values suggesting residual tensile stresses of 228MPa in the cold forged section. While the larger cross section has the A-SP measured fatigue limit the accumulator pipe C-SP itself revealed a 5 million cycles pressure amplitude of 600bar only. This drop of fatigue strength can be largely but not fully explained by tensile residual stresses in the OD14.3/ID10mm section that develop on the bore surface during cold-forging. In top of that enlarged micro-cracks at the end of the transition zone towards the OD14.3/ID7mm pipe section (location 2 in figure 10) may have contributed to that result. The presence of residual tensile stresses is confirmed by finishing cold forged accumulator pipe with a solution annealing treatment (C-SA), which increased the endurable pressure amplitude from 600 to 900bar (safety factor 1.29). It is interesting to note that a solution treatment has the same effect like an autofrettage treatment, whereas the application of an autofrettage treatment after solution annealing did not result in a significant increase in the 5 million cycles pressure amplitude above 900bar. The weak and larger OD20/ID10mm - cross section limits here the applicable autofrettage pressure and becomes the fatigue limiting factor as discussed for sample A-SP-AF.

The strongest gap between calculated and measured flow pressure was observed for the gun drilled and cold forged pipe B with the dimensions OD20/ID10mm. Bearing in mind that the cold forged cross section OD20/ID10mm of sample B has about the same OD/ID-ratio as sample C with OD14.3/ID7mm the difference between these two samples with respect to the measured, remaining residual tensile stress (228MPa vs. 373MPa) is not rational. The estimated residual tensile stress in sample B is so big that virtually no resistance to mechanical fatigue is left. Premature failures at a pressure amplitude of 1100 and 900bar nevertheless suggests that the endurable 5 million cycles pressure amplitude is most likely around 600bar. However, the autofrettage effect resulting from cycle 1 brings the measured flow pressure back to the calculated flow pressure. This is a clear evidence, that the so detrimental residual stresses of tensile nature can be re-distributed by an autofrettage treatment. This is of high relevance because the high strength introduced by cold forging in the smaller ID14.3/7mm as well as in the larger OD20/ID10mm cross section can now be used to increase the autofrettage pressure by a factor of 2 to 3.

Accordingly, work hardening by cold forging enabled accumulator pipe D-AF to increase the autofrettage pressure from 2000 bar to 5000bar, which made it possible to increase the endurable pressure amplitude to 2100bar (safety factor 3).

It appears when looking at the discrepancies between calculated fatigue limits from measured residual stresses and measured 5 million pressure pulsation amplitudes that the proposed pressure-expansion measurements are no accurate enough to detect more localized pressure states in the bore. Unlike tensile samples, where stress-strain relations can be analyzed assuming homogenous stress states and a strain that results from a large aggregated volume, stress states in the pipe are not uniform and there can be steep and changing stress gradients at and just below the bore surface, which apparently can’t be detected by the measurement of macroscopic expansions as applied in this study. While big changes in long-ranging residual stresses can be detected by pipe expansion measurements, the nucleation of fatigue cracks capable to growth is assumed to be sensitively depending on local stress states.

As a summary it has to be concluded that the fatigue strength of pipes made of austenitic stainless steels could be over-estimated by

mechanical integrity calculations. Accordingly, the endurable pressure pulsation amplitude would have to be measured or a higher safety factor would have to be considered in the design of high pressure components made of commercially available austenitic seamless pipes. It also appears that the autofrettage effect in pipes with an OD/ID-ratio of 2 and made of soft austenitic stainless steels is over-estimated by mechanical calculations.

5.2 Materials and process selection for accumulator pipes

It would be interesting to investigate manufacturing and mechanical properties of an accumulator pipe that is made of a normalized carbon steel or soft annealed, low alloyed carbon steel. One relevant advantage of austenitic stainless steels is based on the fact that austenitic stainless steels generally show a stronger work hardening response to cold forging and provide a higher ductility in the work hardened condition than (low alloyed) carbon steels. It is the strength of the material that enables to apply an autofrettage treatment at higher pressures and this study has shown that it is the level of the autofrettage pressure that drives the safety factor in cold formed pipes up-wards. In this respect austenitic stainless steels are expected to provide an advantage over (low alloyed) carbon steels for manufacturing of work hardened components besides their superior corrosion resistance.

5.3 Case hardening

This study has provided further evidence about the beneficial effect of nitrogen in solid solution on pitting corrosion resistance as expressed by the pitting resistance equivalent number PREN (equation 8). The observed enhancement of the pitting corrosion potential in figure 12 goes along with an increase in martensite hardness (figure 11) as expected from the empirical relation between hardness and C+N content (equation 9). It suggests that the solution nitriding process at 1100°C with a nitrogen partial pressure of 1bar is effective. Based on that the achievement of a pitting corrosion resistance comparable to 316L type steels with a case hardenable martensitic stainless steel seems to be achievable. The achievable hardness level in turn seems to be limited today to about 600HV and this is a clear disadvantage to case hardenable carbon steels that reach hardness levels of 700HV. More detailed experimental investigations into the effects of Cr, Ni and C close to the alloy composition of alloy AP2 needs to be carried out in order to understand this limitation. In this study the case hardening depth is around 450microns, but can still be enlarged by increasing the holding time during solution nitriding. The achieved combination of tensile-strength R_m (1365MPa) and elongation A5 (14.7%) is adequate. The strength-ductility balance in the core is by experience most effectively controlled by the carbon and nickel content. In alloy AP2 a reduction of the carbon content is expected to reduce strength and by the way to increase ductility in the core.

6 SUMMARY AND CONCLUSIONS

The use of stainless steels for the manufacturing of fuel system components has been investigated by studying the boundary conditions for design, mechanical behavior, materials and manufacturing. Materials selection, pipe manufacturing and finishing methods like autofrettage and heat treatment have been suggested and experimentally verified to optimize the high pressure performance of fuel system components.

Cold forming of pipes made of 316L stainless steels is shown to be an effective mean to increase the base strength of pipes and to reduce the sealing diameter at high pressure interfaces by reducing the bore diameter at the ends of the fuel lines, whereas the former factor is shown to be relevant for an increased safety factor with respect to mechanical fatigue and sealing at high pressure connections.

It is experimentally verified that cold forming of 316L stainless pipes is a way to maximize fatigue resistance in combination with autofrettage despite the detrimental effects of tensile residual stresses brought in by the cold forming process. This is due to the effect of higher strength that enables the application of much higher autofrettage pressures and the effect of this autofrettage on redistribution of internal stresses and the generation of desired compressive stresses.

For components subject to wear an alloy design of a stainless steel is demonstrated that allows case hardening by solution nitriding up to a surface hardness of 600HV while at the same time enhancing pitting corrosion resistance of the case hardened surface to the level of 316L stainless steels. This nickel alloyed martensitic stainless steel based on Fe-12Cr-3Ni-0.15C provides a very beneficial combination of high strength and ductility in the core of a case hardened product.

7 ACKNOWLEDGMENTS

The authors would like to thank Mr. Peter Fuchs for financial support of this study and his personal commitment to R&D in the field of fuel system components.

8 REFERENCES

[1] Gavriljuk, V.G. and Berns, H. 1999. *High Nitrogen Steels*, Springer, Heidelberg, Germany.

[2] Göcmen A., Wrona F., Ehrensperger J. and Okonji K. 2016. An engine layout study for common rail systems in large diesel engines. Proceedings of *28th CIMAC World Congress*, Helsinki, paper 2016 I 094

[3] Truman, J.E., 1987, *Proceedings of U.K. Corrosion 87, Inst. of Corr. Sci. and Techn.*, Brighton, 111-129

[4] Göcmen A., 2014. An alloy design of a case hardenable ferritic stainless steel, Proceedings of *12th international conference on high nitrogen steels (HNS2014)*, Hamburg

9 CONTACT

Dr. Alkan Goecmen
PETER FUCHS TECHNOLOGY GROUP AG
Im Bilg 8
8450 Andelfingen, Switzerland
alkan.goecmen(at)fuchstechnology.ch
www.fuchstechnology.ch

Dr. Frank Wrona
PETER FUCHS TECHNOLOGY GROUP AG
Im Bilg 8
8450 Andelfingen, Switzerland
frank.wrona(at)fuchstechnology.ch
www.fuchstechnology.ch

Fabian Bartholdi
PETER FUCHS TECHNOLOGY GROUP AG
Im Bilg 8
8450 Andelfingen, Switzerland
fabian.bartholdi(at)fuchstechnology.ch
www.fuchstechnology.ch